

引用格式: 南德斌, 李振宏, 董晓朋, 等, 2023. 运城盆地栲栳塬晚更新世地层序列及地质意义 [J]. 地质力学学报, 29 (4): 497–511.
DOI: [10.12090/j.issn.1006-6616.2023042](https://doi.org/10.12090/j.issn.1006-6616.2023042)

Citation: NAN D B, LI Z H, DONG X P, et al., 2023. Late Pleistocene stratigraphic sequence and geologic significance of the Kaolao Tableland in the Yuncheng Basin [J]. Journal of Geomechanics, 29 (4): 497–511. DOI: [10.12090/j.issn.1006-6616.2023042](https://doi.org/10.12090/j.issn.1006-6616.2023042)

运城盆地栲栳塬晚更新世地层序列及地质意义

南德斌^{1,2,3}, 李振宏^{2,3,4}, 董晓朋^{2,3,4}, 寇琳琳^{2,3,4}, 韦利杰^{2,3,4}

NAN Debin^{1,2,3}, LI Zhenhong^{2,3,4}, DONG Xiaopeng^{2,3,4}, KOU Linlin^{2,3,4}, WEI Lijie^{2,3,4}

1. 中国地质大学(北京)地球科学与资源学院, 北京 100083;
2. 中国地质科学院地质力学研究所, 北京 100081;
3. 自然资源部古地磁与古构造重建重点实验室, 北京 100081;
4. 自然资源部活动构造与地质安全重点实验室, 北京 100081

1. *School of Earth Sciences and Resources, China University of Geosciences (Beijing), Beijing 100083, China;*
2. *Institute of Geomechanics, Chinese Academy of Geological Sciences, Beijing 100081, China;*
3. *Key Laboratory of Paleomagnetism and Tectonic Reconstruction, Ministry of Natural Resources, Beijing 100081, China;*
4. *Key Laboratory of Active Tectonics and Geological Safety, Ministry of Natural Resources, Beijing 100081, China*

Late Pleistocene stratigraphic sequence and geologic significance of the Kaolao Tableland in the Yuncheng Basin

Abstract: The ancient Fen River diversion was a crucial earth's surface transformation in the Yuncheng Basin during the Cenozoic. The time frame for the diversion of the ancient Fen River is still characterized by two views: the middle Pleistocene and the late Pleistocene, which has yet to be finalized. This study investigated the late Pleistocene sedimentary sequence of the Kaolao Tableland in the Yuncheng Basin, and the critical time frame of the sedimentary sequence transition was determined based on optically stimulated luminescence (OSL) dating results. The causes of the late Pleistocene sedimentary sequence of the Kaolao Tableland and the geological factors that controlled the sequence were analyzed using detrital zircon U–Pb isotope dating. It is concluded that the late Pleistocene sedimentary sequence of the Kaolao Tableland in the Yuncheng Basin is characterized by a two-layer structure, with fluvial sands in the lower part and eolian loess in the upper part. Based on the OSL dating results, the formation time of the boundary between these two parts is between ~76–63 ka B.P. Comparative analysis of detrital zircon age sequences indicates that the early Pleistocene fluvial sands in the Kaolao Tableland and sediments in the ancient Fen River have similar age sequence characteristics. Therefore, it can be deduced that the regional tectonic uplift of the northeastern Emei Terrace in the middle of the late Pleistocene resulted in the diversion and exit of the ancient Fen River from the Yuncheng Basin and the sedimentary facies began to change from fluvial to eolian. The tectonic uplift in the middle of the late Pleistocene extensively developed around the Ordos Basin, and that indicates a significant tectonic uplift of the Tibet Plateau during this time, whose remote effect might be the major cause for the exit of the ancient Fen River from the Yuncheng Basin. This research provides new sedimentary evidence for the time frame of the ancient Fen River diversion in the Yuncheng Basin.

Keywords: fluvial facies; eolian loess; ancient Fen River; late Pleistocene; Yuncheng Basin; Zircon U–Pb ages

基金项目: 中国地质调查局地质调查项目 (DD20221644, DD20190018); 国家自然科学基金项目 (41972119, 41702216)

This research is financially supported by the Geological Investigation Project of the China Geological Survey (Grants DD20221644 and DD20190018) and the National Natural Science Foundation of China (Grants No. 41972119 and 41702216).

第一作者: 南德斌 (2000—), 男, 在读硕士, 从事沉积地质与大地构造方面的研究工作。E-mail: nandebin@163.com

通讯作者: 李振宏 (1973—), 男, 研究员, 从事沉积地质与大地构造方面的研究工作。E-mail: lizhenhong@126.com

收稿日期: 2023-03-28; 修回日期: 2023-05-28; 责任编辑: 范二平

摘要: 古汾河改道是运城盆地新生代时期一次重要的地表巨变过程, 对于古汾河改道时限目前仍存在着中更新世和晚更新世2种观点, 尚未有统一的定论。研究以运城盆地栲栳塬晚更新世沉积序列为调查对象, 在光释光测年的基础上, 厘定了沉积序列转换的关键时限; 结合碎屑锆石 U-Pb 同位素测年, 分析了栲栳塬晚更新世沉积序列的成因及地质主控因素。研究认为: 运城盆地栲栳塬晚更新世沉积序列具有双层结构的特点, 下部为一套河流相砂体, 上部为一套风成相黄土, 二者之间的界限大约在 7.6~6.3 万年; 碎屑锆石年龄序列对比分析认为, 栲栳塬晚更新世早期的河流相沉积与运城盆地汾河古河道的沉积特征基本一致, 晚更新世中期, 由于峨眉台地的区域性抬升, 古汾河发生改道进而退出运城盆地, 栲栳塬早期的河流相沉积之上开始接受持续的风成相沉积; 运城盆地晚更新世中期的构造抬升事件在鄂尔多斯盆地周缘均有响应, 预示着青藏高原在该时期存在一期明显的构造隆升, 其远程效应是造成汾河改道退出运城盆地的主要动力。该研究成果从沉积角度为运城盆地古汾河的改道时限提供了新的证据。

关键词: 河流相; 风成黄土; 古汾河; 晚更新世; 运城盆地; 锆石 U-Pb 年龄

中图分类号: P534.631 **文献标识码:** A **文章编号:** 1006-6616 (2023) 04-0497-15

DOI: 10.12090/j.issn.1006-6616.2023042

0 引言

运城盆地位于鄂尔多斯盆地东南部, 汾渭地堑系的核心部位, 隶属于近东西向渭河盆地与近北东向山西地堑系的过渡部位, 接受了汾渭地堑系新生代最早的沉积(王强等, 2000; 韩恒悦等, 2001, 2002; 邢作云等, 2005; 李智超等, 2015, 2016; 李兆雨等, 2021; 秦帮策等, 2021)。新生代时期, 该区域经历了三门古湖消亡、黄河贯通三门峡东流入海等多期构造地貌的巨变过程, 进而控制着盆地内及相邻地区河湖体系的演化(吴锡浩等, 1998; 潘保田等, 2005; Jiang et al., 2007; 张磊等, 2018; Shang et al., 2018; 闫纪元等, 2021; 胡健民等, 2022)。古汾河退出运城盆地, 经现今的河津一带注入黄河, 这一流路的变化就是其中一次重要的古地貌变化过程(胡晓猛, 1997; 孙继敏和许立亮, 2007; 胡小猛等, 2010, 2012; 索艳慧等, 2012, 2017; 李三忠等, 2013, 2019)。研究认为, 运城盆地早更新世与中更新世早中期, 汾河古河道在盆地内的分布情况基本一致, 主要沿着峨眉台地稷王山与孤山之间、隘口—礼元镇之间2个分支注入运城盆地, 在运城盆地内呈现辫状河分布。中更新世晚期, 古汾河的2个分支相继退出了运城盆地(胡晓猛, 1997)。另一种观点主要根据运城盐湖盐层的发育情况推断汾河河道自晚更新世时期退出了运城盆地, 运城盐湖的地表水补给明显减少, 中条山山前汇水盆地逐渐进入封闭体系, 盐类矿物开始沉积(李有利等, 1994)。关于汾河改道退出运城盆地的时限, 由于盆地内地表覆盖较为严

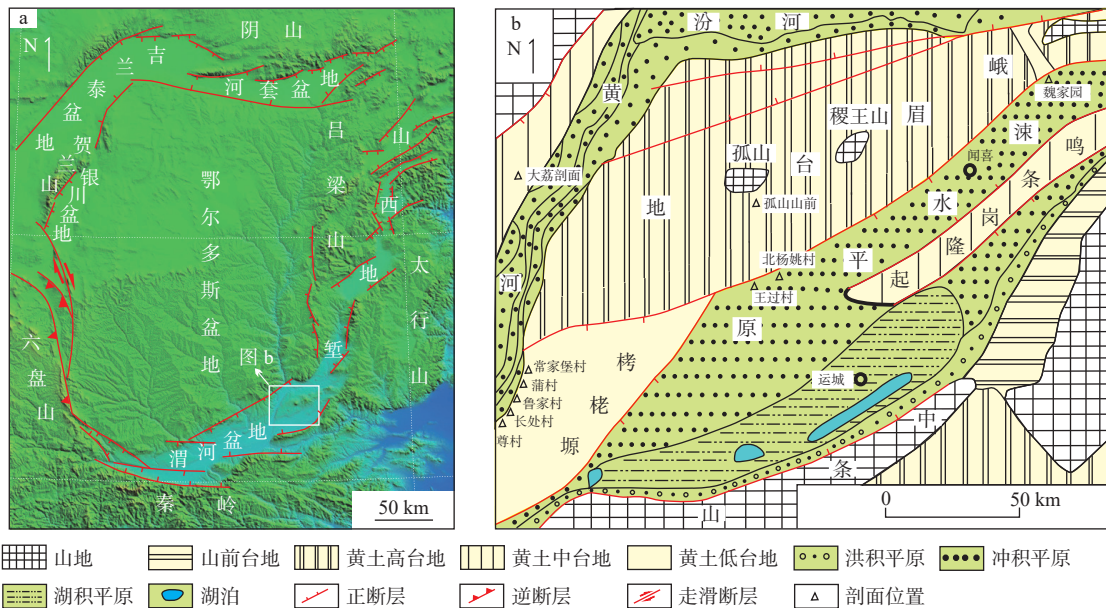
重, 人为扰动较大, 仅有的露头剖面也仅仅出露于峨眉台地、鸣条岗隆起附近的局部高地, 认识相对比较局限。目前针对古汾河改道时限, 主要存在着中更新世和晚更新世2种观点, 尚未得出统一的结论(郭令智和薛禹群, 1958; 李有利等, 1994; 胡晓猛, 1997)。此次研究以运城盆地栲栳塬晚更新世沉积序列演化为主线, 通过盆地内沉积序列的变化时限、沉积物源的示踪来分析沉积序列变化的主控因素, 进而演绎古汾河河道退出运城盆地的时限, 研究成果将从沉积角度为古汾河河道的变迁过程提供最新的证据。

1 区域地质概况

运城盆地是山西地堑系西南端的一个断陷盆地, 主要包括峨眉台地、涑水平原、栲栳塬和鸣条岗隆起4个次级构造地貌单元(图1)。峨眉台地位于运城盆地北部, 其南北两侧均有陡坎, 呈现北东—南西走向, 延伸长约60 km, 宽约25 km, 除了孤山、稷王山外, 其余均为巨厚黄土覆盖, 顶面比较平坦(李振宏等, 2020a)。野外露头和钻孔资料揭示, 峨眉台地主要由中更新世离石黄土和晚更新世马兰黄土组成, 黄土下伏有晚新生代河湖相沉积和古生代寒武系鲕粒灰岩以及石炭系含煤层系。稷王山位于峨眉台地中段, 海拔为1281 m, 山体主要由寒武系鲕粒灰岩和太古界片麻岩组成; 孤山山体海拔为1411.2 m, 全部由早白垩世花岗岩组成, 可能代表了中生代华北克拉通破坏已经影响到了运城盆地(齐玥等, 2011, 2016)。涑水平原地势由北向南逐

渐降低,中条山北麓盐池一带最低,海拔约320 m,低于邻近的黄河枯水面20余米。盆地内部可以进一步分为次一级地貌单元,盆地中部有1个北东—南西走向,东起中条山地,西至王范、北相一带的长条状高地,称之为鸣条岗。鸣条岗主要由早更新世以来的河湖相地层及第四纪中晚期的黄土组成。在岗地的东南侧和西北侧均有正断层发育,说明鸣条岗为盆地中的小地垒。涑水平原主体为一套河湖相沉积组成,在南部的中条山山前发育一套全新

世的冲积扇,向盆地内部逐步过渡到以运城盐湖为中心的湖积平原沉积,鸣条岗隆起与峨眉台地地层发育特征基本相同,在三门古湖上沉积中更新世离石黄土及晚更新世马兰黄土。栲栳塬夹持于涑水平原与峨眉台地之间,为一黄土低台地地貌单元,钻井序列揭示早更新世至晚更新世中期,其为一套连续的河湖相沉积,河道砂体发育,晚更新世中晚期至全新世为一套风成黄土沉积(图2)。



a—区域构造位置图; b—构造地貌划分图

图1 研究区构造位置与构造地貌划分

Fig. 1 Tectonic background and landforms of the study area

(a) Tectonic background and location of the study area; (b) Tectonic landforms

2 样品采集与分析

2.1 样品采集

实验样品主要采集于运城盆地栲栳塬晚更新世尊村剖面(图1,图2)。尊村晚更新世剖面岩性特征在露头上可以划分为上、下2部分,二者之间的接触关系具有明显的由水成向风成过渡的相变关系(图3a)。下部岩性为1套中厚层状浅灰白色、浅棕红色细砂、含砾粗砂夹浅紫红色薄层黏土、粉砂质黏土和黏土质粉砂,局部发育小型斜层理及沙纹层理,含大量虫孔及石膏斑晶(图3b),总体反应了一套干旱环境下的河流相沉积特征,局部可能受到构造运动的扰动;上部岩性总体上为1套浅灰白色

厚层状黄土,局部偶见柱状节理,中上部夹有1套厚度约1.5 m的棕红色古土壤层,横向上比较连续,在整个栲栳塬具有区域可对比性,含植物化石碎屑及虫孔,区域上具有风成马兰黄土的典型特征,剖面总体厚度约为20.5 m。为了建立尊村剖面的地层年代格架,在剖面的底部浅灰—白色粉砂层、中部河流相砂与黄土的过渡部位以及上部古土壤层的底部共采集光释光样品3个。同时,在涑水平原王过村剖面地层角度不整合面上下分别采集了2个光释光样品,来大致限定不整合面上下地层的年龄,为不整合界面的形成时代提供参考(图3c);在涑水平原北杨姚村剖面晚更新世丁村组和峙峪组分别采集2个光释光样品,以确定二者界面之间的时限(图3d)。通过尊村剖面、王过村剖面、北杨姚村地

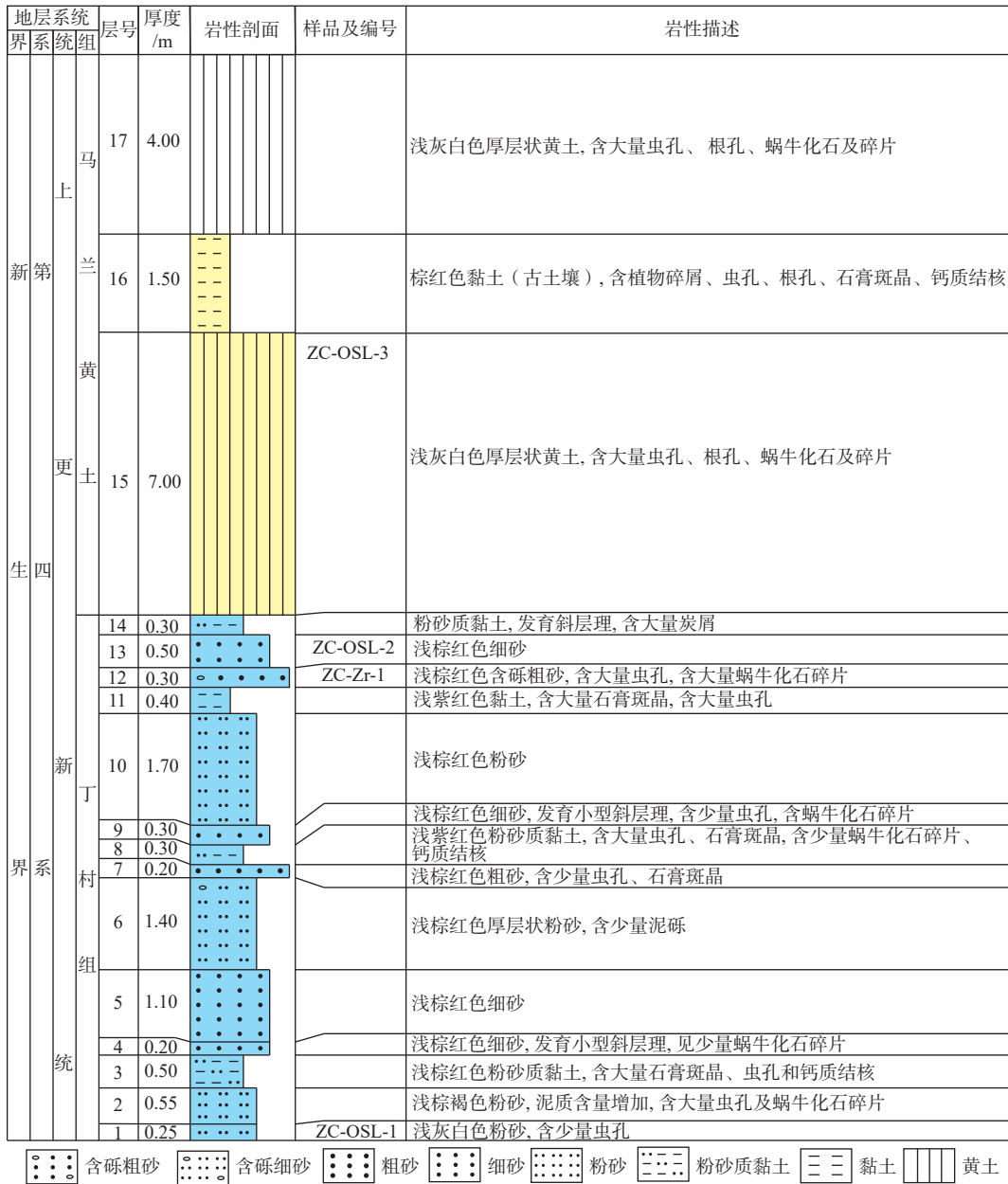
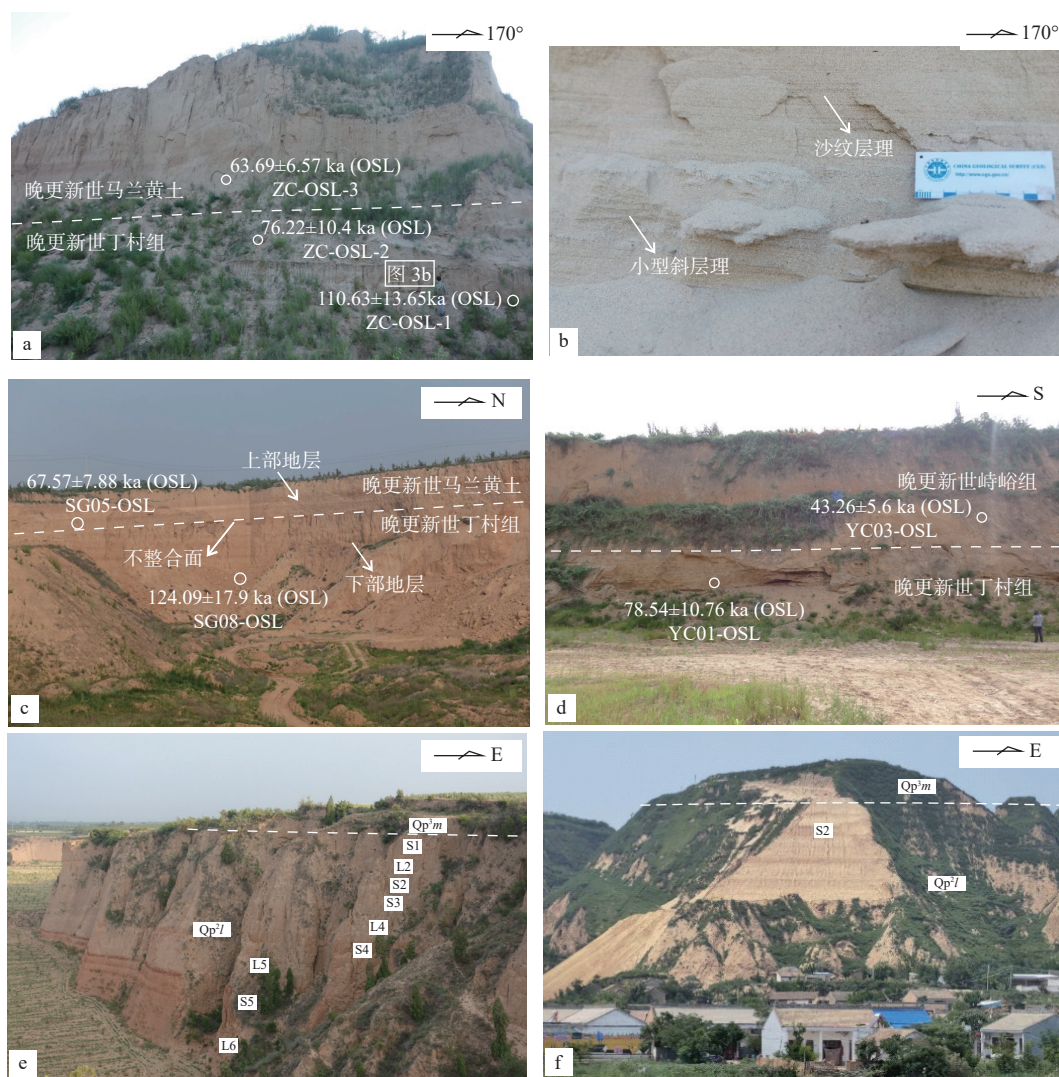


图 2 尊村晚更新世剖面地层特征
Fig. 2 Late Pleistocene stratigraphic sequence in the Zuncun section

层剖面建立涑水平原晚更新世地层对比格架。光释光样品的采集工作首先在剖面上选取岩性比较均匀的细粉砂及黄土部位, 然后用铲子去除表面 30~50 cm 厚度的风化部分, 针对新鲜未风化的样品用钢管取样, 在钢管取出样品后, 立刻用黑塑料袋包裹严实, 避免阳光的照射。此次研究还在尊村剖面中部河流砂中采集碎屑锆石 U-Pb 年代学测试样品 1 件(样品编号 ZC-Zr-1; 图 2), 开展古汾河河道的溯源对比工作。同时, 离石黄土中明显标志层 S2、S5 也为地层年代格架限定提供了依据(图 3e、3f)。

2.2 实验分析

光释光样品的测年工作在中国地震局地壳应力研究所地壳动力学重点实验室完成。采集的样品先在实验室去除钢管顶部和底部可能曝光、污染的部分, 主要保留钢管中心部位的样品来进行等效剂量的测定; 从中取出约 20 g 样品测定含水量和饱和含水量, 之后将样品烘干、充分研磨, 直至全部通过 63 μm 的筛子, 选取 4~11 μm 细颗粒组分进行处理, 光释光辐照和信号测量在丹麦 Risoe DA-20-C/D 型热/光释光自动测量系统上完成; 同时, 取部分样品在核工业北京地质研究所测定其 U、Th、



图例
 Qp^{3m}—马兰组; Qp^{2l}—离石组; S1、L2、S2、S3、L4、S4、L5、S5、L6—古土壤层

a、b—栲栳塬尊村晚更新世剖面; c—涑水平原王过村晚更新世剖面; d—涑水平原北杨姚村晚更新世剖面; e—峨眉台地孤山山前离石-马兰黄土剖面; f—峨眉台地大荔离石-马兰黄土剖面

图 3 运城盆地第四系典型剖面特征

Fig. 3 Typical Quaternary sections in the Yuncheng Basin

(a and b) Late Pleistocene stratigraphic sequence in the Zuncun section of the Kaolao Tableland; (c) Late Pleistocene stratigraphic sequence in the Wangguocun section of the Sushui Plain; (d) Late Pleistocene stratigraphic sequence in the Beiyangyaocun section of the Sushui Plain; (e) Lishi-Malan loess stratigraphic sequence at the front of Gushan Mountain in the Emei Terrace; (f) Lishi-Malan loess stratigraphic sequence in the Dali section in the Emei Terrace

K 含量, 其中 U、Th 含量用 NexION300D 等离子体质谱仪测定, K 含量用 Z-2000 石墨炉原子吸收分析仪测定。由于实验中样品的细颗粒石英未进行 α 系数 (即 α 辐射产生释光信号的有效系数) 的测量, 在计算年龄时, α 系数采用 0.045 ± 0.005 (崔加伟等, 2018; 仇度伟等, 2021)。

碎屑锆石 U-Pb 同位素测年样品碎样与锆石挑选、制靶、阴极发光以及透射、反射照相工作均由

河北省区域地质调查研究院测试分析实验室完成; LA-ICP-MS 锆石微区 U-Pb 同位素测定在自然资源部古地磁与古构造重建重点实验室分析完成。此次分析的数据采用软件 ICPMSDataCal (Liu et al., 2008, 2010a) 进行离线处理, 实验仪器操作过程和数据处理方法具体见 Liu et al. (2008, 2010a, 2010b)。锆石 U-Pb 同位素定年中采用锆石标准 91500 作外标来进行同位素分馏校正, 在测试过程中, 每分析

6个样品点,需要分析2次锆石标准91500和1次Ple。对于与分析时间有关的U-Th-Pb同位素比值漂移,利用锆石标准91500的变化采用线性内插的方式进行了校正,数据处理方法见Liu et al.(2008)。锆石标准91500的U-Th-Pb同位素比值推荐值据Wiedenbeck et al.(1995)。锆石样品的U-Pb年龄谱和图绘制和年龄权重平均计算均采用Isoplot/Ex_ver3完成(Ludwig, 2003)。

3 实验结果

根据光释光测年结果分析(表1),尊村剖面底部浅灰—白色粉砂岩层样品的测试年龄为110.63±13.65 ka,中部河流相砂与黄土的过渡部位的样品测试年龄为76.22±10.4 ka,上部古土壤底部样品测试年龄为63.69±6.57 ka;王过村剖面角度不整合面上下2个光释光样品的年龄分别为124.09±17.90 ka和

67.57±7.88 ka;北杨姚村剖面晚更新世丁村组和峙峪组的样品测试年龄分别为78.54±10.76 ka和43.26±5.60 ka。尊村剖面的3个光释光样品自下而上的年龄依次变小,并没有发现年龄倒转的现象。

碎屑锆石U-Pb同位素测年有效点的分析主要选取谐和率>90%的样品点,测试结果见表2。共测试样品点102个,其中有效样品点97个。碎屑锆石阴极发光图像显示,锆石形态大多数呈现椭圆形,颜色较深,个别具有细小的变质边,部分样品自形较好,岩浆环带清晰(图4)。锆石颗粒中等,一般大小为100~200μm,仅有少部分锆石的颗粒小于100μm。锆石Th/U比值介于0.06~5.19,比值小于0.4的约占30%。锆石的整体年龄序列存在11个比较明显的峰值,分别为126 Ma、275 Ma、291 Ma、359 Ma、429 Ma、460 Ma、803 Ma、926 Ma、1855 Ma、2466 Ma和2522 Ma(图5)。

表1 光释光样品年龄测试结果

Table 1 Optically stimulated luminescence ages

序号	野外编号	U/ (μg/g)	Th/ (μg/g)	K/ %	测试粒径/ μm	测试方法	环境剂量率/ (Gy/ka)	等效剂量/ Gy	年龄/ ka
1	ZC-OSL-1	1.61	6.90	1.87	4~11	SMAR	2.92±0.22	323.51±31.98	110.63±13.65
2	ZC-OSL-2	2.52	10.80	1.83	4~11	SMAR	3.55±0.25	270.25±31.45	76.22±10.40
3	ZC-OSL-3	2.46	11.50	1.66	4~11	SMAR	3.46±0.24	220.04±16.64	63.69±6.57
4	YC03-OSL	2.76	12.30	1.60	4~11	SMAR	4.15±0.25	179.36±14.76	43.26±5.60
5	YC01-OSL	1.93	9.71	1.86	4~11	SMAR	3.82±0.23	300.26±28.10	78.54±10.76
6	SG05-OSL	11.00	12.40	1.86	4~11	SMAR	7.53±0.22	508.89±0.58	67.57±7.88
7	SG08-OSL	1.90	7.09	2.09	4~11	SMAR	3.77±0.21	467.56±48.60	124.09±17.90

表2 ZC-Zr-1 样品碎屑锆石年龄测试结果

Table 2 U-Pb ages of detrital zircons from the sample ZC-Zr-1

测试点号	含量/×10 ⁻⁶			同位素比值				年龄/Ma			
	Pb	Th	U	²⁰⁷ Pb/ ²³⁵ U	1σ	²⁰⁶ Pb/ ²³⁸ U	1σ	²⁰⁷ Pb/ ²⁰⁶ Pb	1σ	²⁰⁶ Pb/ ²³⁸ U	1σ
ZC-Zr-1	178.0	222.0	199	11.0402	0.1939	0.4822	0.0049	2509	29	2537	21
ZC-Zr-3	31.1	268.0	638	0.2821	0.0071	0.0386	0.0003	320	57	244	2
ZC-Zr-4	19.6	115.0	226	0.5196	0.0144	0.0678	0.0006	435	63	423	4
ZC-Zr-5	8.5	64.1	111	0.3331	0.0159	0.0442	0.0006	433	145	279	4
ZC-Zr-6	7.0	62.8	103	0.2817	0.0168	0.0404	0.0006	250	139	255	4
ZC-Zr-7	160.0	155.0	247	9.1073	0.1536	0.4299	0.0035	2383	29	2305	16
ZC-Zr-8	6.9	75.3	114	0.3095	0.0172	0.0426	0.0005	328	119	269	3
ZC-Zr-9	54.9	14.1	102	10.4488	0.1983	0.4628	0.0043	2492	31	2452	19
ZC-Zr-10	13.2	68.4	132	0.5638	0.0219	0.0741	0.0008	413	83	461	5
ZC-Zr-11	55.5	31.7	139	5.9408	0.1088	0.3519	0.0031	1990	38	1944	15
ZC-Zr-12	215.5	54.2	670	5.1155	0.0827	0.3243	0.0030	1866	27	1810	15

续表 2

测试点号	含量/ $\times 10^{-6}$			同位素比值				年龄/Ma			
	Pb	Th	U	$^{207}\text{Pb}/^{235}\text{U}$	1σ	$^{206}\text{Pb}/^{238}\text{U}$	1σ	$^{207}\text{Pb}/^{206}\text{Pb}$	1σ	$^{206}\text{Pb}/^{238}\text{U}$	1σ
ZC-Zr-13	6.0	69.8	93	0.3093	0.0184	0.0443	0.0007	300	147	279	4
ZC-Zr-14	27.1	24.4	67	5.1031	0.1029	0.3287	0.0030	1843	38	1832	14
ZC-Zr-15	55.0	92.1	99	5.0927	0.1013	0.3252	0.0030	1854	41	1815	14
ZC-Zr-16	232.0	601.0	275	4.8464	0.0892	0.3108	0.0024	1842	33	1745	12
ZC-Zr-17	42.5	34.2	108	5.2593	0.0967	0.3294	0.0027	1890	35	1835	13
ZC-Zr-18	69.9	119.0	410	1.5147	0.0254	0.1545	0.0012	954	35	926	6
ZC-Zr-19	87.5	154.0	166	4.5015	0.0811	0.3013	0.0027	1769	33	1698	14
ZC-Zr-20	250.0	202.0	415	9.2668	0.1540	0.4139	0.0044	2474	24	2233	20
ZC-Zr-21	87.9	84.1	132	9.0100	0.1552	0.4541	0.0051	2272	27	2414	22
ZC-Zr-22	33.0	34.5	64	6.4872	0.1475	0.3737	0.0041	2037	39	2047	19
ZC-Zr-23	271.0	52.5	590	8.8208	0.1462	0.4171	0.0037	2379	28	2247	17
ZC-Zr-24	242.0	148.0	389	10.4343	0.1845	0.4769	0.0044	2437	30	2514	19
ZC-Zr-25	51.9	51.9	72	9.4711	0.1963	0.4489	0.0047	2377	35	2390	21
ZC-Zr-26	145.5	72.3	251	10.4246	0.1710	0.4677	0.0041	2466	28	2474	18
ZC-Zr-27	106.8	146.0	150	7.7183	0.1212	0.3885	0.0032	2272	27	2116	15
ZC-Zr-28	151.0	190.0	160	10.9927	0.1621	0.4756	0.0038	2529	25	2508	17
ZC-Zr-29	117.6	123.0	147	10.5719	0.1535	0.4671	0.0041	2495	26	2471	18
ZC-Zr-30	104.2	97.9	246	5.3593	0.0908	0.3345	0.0032	1892	30	1860	15
ZC-Zr-31	94.4	126.0	111	9.4867	0.1727	0.4453	0.0042	2391	31	2374	19
ZC-Zr-33	30.0	40.9	60	4.8823	0.1041	0.3259	0.0029	1768	39	1818	14
ZC-Zr-34	89.3	111.0	117	8.7490	0.1420	0.4248	0.0032	2332	29	2282	14
ZC-Zr-35	79.6	69.0	182	5.9436	0.1270	0.3477	0.0051	2006	30	1924	24
ZC-Zr-36	149.0	203.0	301	5.0792	0.0822	0.3330	0.0028	1811	28	1853	13
ZC-Zr-37	118.0	86.5	209	8.6450	0.1388	0.4113	0.0030	2365	27	2221	14
ZC-Zr-38	305.0	170.0	519	9.8174	0.1598	0.4553	0.0041	2409	27	2419	18
ZC-Zr-39	16.8	165.0	226	0.3800	0.0130	0.0499	0.0006	428	80	314	4
ZC-Zr-40	88.7	49.1	144	10.6158	0.2174	0.4693	0.0047	2490	33	2481	21
ZC-Zr-42	23.1	327.0	339	0.2811	0.0087	0.0398	0.0004	254	68	252	3
ZC-Zr-43	72.4	65.8	176	5.1621	0.0965	0.3275	0.0030	1862	34	1826	14
ZC-Zr-44	68.6	45.6	215	4.3364	0.0796	0.2955	0.0028	1732	33	1669	14
ZC-Zr-45	42.5	63.0	82	4.9999	0.1002	0.3271	0.0030	1806	35	1824	15
ZC-Zr-46	81.1	49.9	263	4.8733	0.1316	0.2961	0.0056	1931	31	1672	28
ZC-Zr-48	20.8	176.0	368	0.3247	0.0107	0.0434	0.0004	372	74	274	2
ZC-Zr-49	352.0	220.0	855	5.7795	0.0953	0.3542	0.0029	1926	30	1955	14
ZC-Zr-50	205.0	161.0	317	10.3477	0.1869	0.4496	0.0042	2522	29	2393	19
ZC-Zr-51	45.2	91.0	61	5.8441	0.1351	0.3509	0.0036	1973	41	1939	17
ZC-Zr-52	150.0	130.0	357	5.7726	0.0950	0.3524	0.0032	1936	26	1946	15
ZC-Zr-53	59.9	77.4	69	10.3819	0.2011	0.4559	0.0048	2508	31	2421	21
ZC-Zr-54	173.5	114.0	440	5.5781	0.0857	0.3453	0.0026	1910	26	1912	12
ZC-Zr-55	256.0	217.0	611	5.8320	0.0968	0.3474	0.0030	1989	28	1922	14
ZC-Zr-56	122.5	117.0	174	9.7395	0.1684	0.4618	0.0043	2376	27	2447	19
ZC-Zr-57	54.8	41.8	99	8.7842	0.1904	0.4025	0.0044	2433	39	2181	20
ZC-Zr-58	210.0	258.0	692	3.7252	0.0818	0.2509	0.0032	1754	33	1443	16
ZC-Zr-59	109.9	71.9	310	4.9964	0.0911	0.3158	0.0028	1873	33	1769	14

续表 2

测试点号	含量/ $\times 10^{-6}$			同位素比值				年龄/Ma			
	Pb	Th	U	$^{207}\text{Pb}/^{235}\text{U}$	1σ	$^{206}\text{Pb}/^{238}\text{U}$	1σ	$^{207}\text{Pb}/^{206}\text{Pb}$	1σ	$^{206}\text{Pb}/^{238}\text{U}$	1σ
ZC-Zr-60	159.4	52.4	455	5.8807	0.1222	0.3431	0.0043	2009	25	1902	21
ZC-Zr-61	63.2	118.0	92	5.8926	0.1198	0.3513	0.0032	1974	35	1941	15
ZC-Zr-62	7.4	68.9	143	0.3139	0.0156	0.0427	0.0006	350	113	270	3
ZC-Zr-63	22.9	47.4	40	4.3841	0.1139	0.3076	0.0033	1688	51	1729	16
ZC-Zr-64	41.5	66.9	80	5.1611	0.1066	0.3291	0.0030	1857	39	1834	15
ZC-Zr-65	83.4	125.0	95	9.2125	0.1785	0.4353	0.0037	2377	34	2329	16
ZC-Zr-66	9.5	75.8	186	0.3220	0.0133	0.0421	0.0005	428	88	266	3
ZC-Zr-68	5.0	62.4	58	0.3527	0.0229	0.0461	0.0007	487	156	290	5
ZC-Zr-69	77.4	118.0	157	5.1547	0.1026	0.3174	0.0038	1915	34	1777	19
ZC-Zr-70	36.3	4.9	86	7.6336	0.1864	0.3970	0.0047	2206	39	2155	22
ZC-Zr-71	31.4	446.0	357	0.3435	0.0122	0.0463	0.0005	339	78	292	3
ZC-Zr-72	35.2	61.8	67	5.2428	0.1118	0.3185	0.0028	1943	40	1782	14
ZC-Zr-73	208.0	194.0	304	9.8833	0.1682	0.4546	0.0040	2433	31	2416	18
ZC-Zr-74	196.3	109.0	357	9.3918	0.1663	0.4410	0.0038	2387	31	2355	17
ZC-Zr-75	154.1	77.1	419	5.4923	0.0902	0.3406	0.0030	1902	31	1890	14
ZC-Zr-76	59.6	181.0	35	5.1197	0.1492	0.3317	0.0042	1828	53	1847	20
ZC-Zr-77	180.0	164.0	231	11.3982	0.1651	0.4871	0.0045	2547	25	2558	20
ZC-Zr-78	100.3	143.0	189	5.5238	0.0798	0.3460	0.0028	1881	26	1916	13
ZC-Zr-79	66.7	97.2	131	5.1919	0.0913	0.3367	0.0031	1817	30	1871	15
ZC-Zr-80	148.0	256.0	249	5.3470	0.0685	0.3361	0.0026	1872	20	1868	13
ZC-Zr-81	261.8	44.0	502	10.8036	0.0939	0.4687	0.0028	2517	12	2478	12
ZC-Zr-82	91.2	56.7	172	8.6002	0.1040	0.4248	0.0031	2298	17	2282	14
ZC-Zr-83	75.2	101.0	137	5.9456	0.0797	0.3577	0.0030	1955	22	1971	14
ZC-Zr-84	33.8	52.4	64	5.1114	0.0910	0.3308	0.0034	1833	34	1842	17
ZC-Zr-85	28.2	130.0	120	1.1959	0.0293	0.1327	0.0012	787	54	803	7
ZC-Zr-86	52.5	78.4	51	10.1950	0.1988	0.4567	0.0049	2473	33	2425	22
ZC-Zr-87	49.1	36.2	126	5.3148	0.0934	0.3371	0.0028	1865	33	1873	14
ZC-Zr-88	58.5	76.5	64	10.3817	0.1800	0.4674	0.0041	2465	30	2472	18
ZC-Zr-89	152.1	43.4	600	3.6819	0.0564	0.2603	0.0019	1665	28	1492	10
ZC-Zr-90	81.2	88.8	175	5.6034	0.1152	0.3492	0.0039	1896	35	1931	19
ZC-Zr-91	172.2	42.8	548	4.9117	0.1059	0.3012	0.0035	1924	35	1697	17
ZC-Zr-92	114.9	86.5	188	9.4665	0.1569	0.4502	0.0039	2372	28	2396	17
ZC-Zr-93	7.6	207.0	249	0.1381	0.0077	0.0198	0.0003	256	131	126	2
ZC-Zr-94	14.3	124.0	271	0.3047	0.0118	0.0434	0.0005	254	88	274	3
ZC-Zr-95	9.5	95.8	103	0.4088	0.0210	0.0574	0.0008	287	122	360	5
ZC-Zr-96	44.0	48.1	105	4.8837	0.0924	0.3297	0.0031	1755	35	1837	15
ZC-Zr-97	89.4	37.5	221	6.2711	0.1077	0.3753	0.0038	1972	62	2054	18
ZC-Zr-98	42.4	65.1	108	4.0810	0.0914	0.2842	0.0037	1694	37	1612	19
ZC-Zr-99	84.8	111.0	184	5.1797	0.0918	0.3282	0.0026	1866	31	1830	13
ZC-Zr-100	13.4	85.8	165	0.4931	0.0197	0.0646	0.0007	443	93	403	4
ZC-Zr-101	10.5	126.0	160	0.3281	0.0156	0.0425	0.0006	461	107	269	4
ZC-Zr-102	16.9	131.0	298	0.3390	0.0128	0.0477	0.0006	333	89	301	4

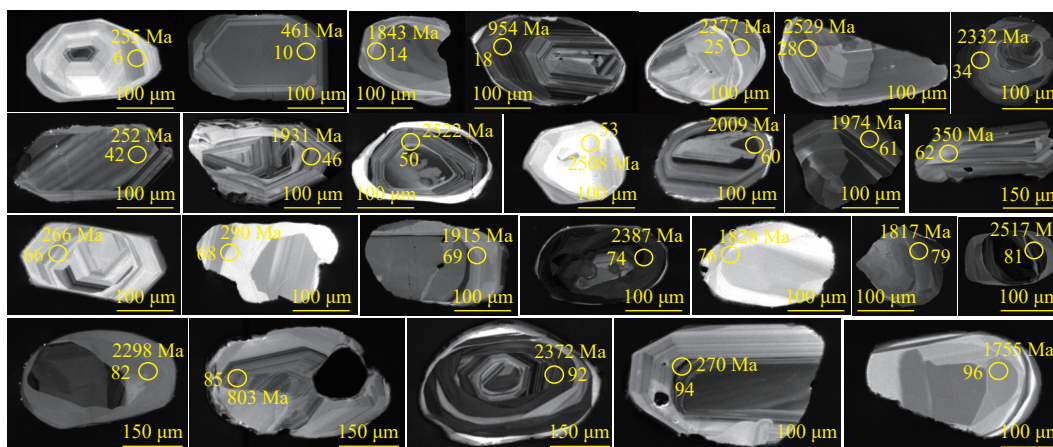
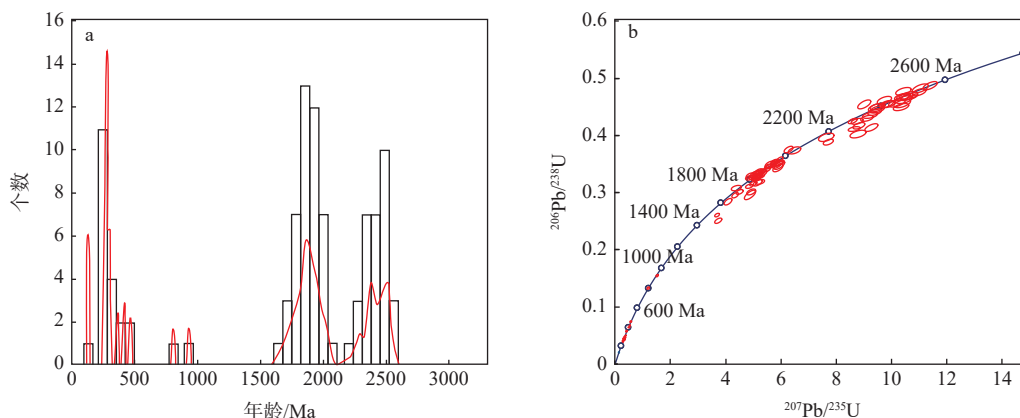


图 4 ZC-Zr-1 样品碎屑锆石典型阴极发光照片

Fig. 4 Typical cathodoluminescence photos of the detrital zircons from the sample ZC-Zr-1



a—碎屑锆石年龄序列; b—碎屑锆石年龄谐和图

图 5 ZC-Zr-1 样品碎屑锆石 U-Pb 年龄序列与年龄谐和图

Fig. 5 Detrital zircon U-Pb age sequence histogram and concordia diagram of the sample ZC-Zr-1

(a) Detrital zircon U-Pb age sequence histogram; (b) Detrital zircon U-Pb age concordia diagram

4 讨论

4.1 古汾河改道时限

运城盆地次级构造单元栲栳塬介于峨眉台地与涑水平原之间, 仅分布在黄河与运城盆地的交界部位, 晚更新世地层具有下部为河流相沉积、上部为风成黄土沉积的地质结构。这种由早期的河流相相变为晚期风成黄土相的沉积过程, 预示着先存河流的消亡、原地接受的风成黄土才得以保存的过程。河流的消亡过程一般存在 2 种主要原因: ①区域上气候环境发生变化, 由温暖湿润的环境转变为寒冷干燥的气候环境, 河流随之自然消亡, 如位于鄂尔多斯高原北部萨拉乌苏河消亡就是这种原因(靳鹤龄等, 2006, 2007); ②由于构造抬升作用, 原有

的河流在某处突然改道, 先期存在的河流逐渐干枯, 风成黄土能够在原来的废弃的河道中得以保存, 如同黄河在演化过程中受到新构造运动的控制而发生多期改道一样, 原有的河道被废弃(徐海亮和王朝栋, 2010)。运城盆地典型的第四系黄土剖面主要见于相邻的峨眉台地以及涑水平原东北部的鸣条岗隆起, 标准剖面见于峨眉台地吴王渡口附近(姚文兵等, 2004)。在吴王渡口剖面, 三门组湖相沉积与中更新世离石黄土平行不整合接触, 在剖面上可以见到明显的 S8 古土壤, 说明在区域上自中更新世开始, 三门古湖退出运城盆地以来, 运城盆地整体处于相对干冷的气候环境, 而且从未发生过明显的变化, 特别是在晚更新世以来, 黄土剖面连续沉积, 也说明栲栳塬河流沉积的突然消失并非区域气候环境的突然变化引起的(安芷生和刘晓东,

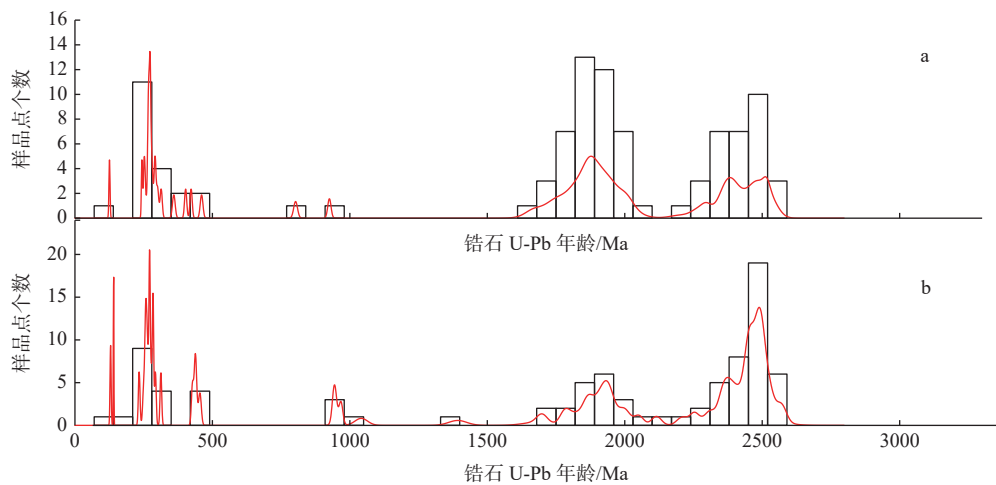
2000; 李振宏等, 2020a)。那么, 这种变化最可能的就是由于原有的河流改道, 古河道突然废弃, 飘落在原有河流中的风成黄土沉积得以保存而造成的。根据光释光的测年结果显示, 这种相变突然发生的时限, 也就是该期区域构造事件发生的时限介于 $76.22 \pm 10.4 \sim 63.69 \pm 6.57$ ka。已有研究在峨眉台地北东方向地表剖面可以见到 S2 古土壤被明显抬升至地表剥蚀, 说明在 S2 古土壤沉积之后, 区域上存在一期明显的构造抬升(李有利等, 1994)。但由于 S2 之上的地层被剥蚀殆尽, 从露头剖面上仅能限定该期构造活动发生于 S2 沉积之后, 而不能限定其具体时限。此次结合栲栳源地层序列的研究结果, 将该期构造活动限定于晚更新世中期, 在该时期原来流经运城盆地的古汾河河道发生了改道, 从而退出运城盆地。根据栲栳源河流相砂岩与峨眉台地魏家园剖面古汾河河道砂岩碎屑锆石测年序列的对比结果分析, 二者在年龄序列上基本保持一致。其中, 126 Ma 年龄峰值主要来自于运城—临汾盆地广泛存在的白垩纪花岗岩, 600~1000 Ma 的年龄峰值可能与区域马兰黄土的沉积存在一定的联系, 而并非是河流源区带来的产物, 其他年龄的峰值都是华北克拉通典型的年龄峰值, 进一步说明栲栳源河流相砂岩是由曾经流经运城盆地的古汾河河道沉积而成的(图 6; 闫纪元, 2021)。另外, 位于运城盆地涑水平原的鸣条岗隆起与峨眉台地在深部构造上同时受到 2 条深大断裂控制, 自早更新世至晚更新世早期, 鸣条岗隆起经历了多期活动, 自北东向南西方向不断抬升, 隆起范围不断扩大, 该隆起的活动性也证明了运城盆地在晚更新世早期发生了一期快速的隆升, 峨眉台地与鸣条岗隆起具有相同的活动背景(李有利等, 1994)。

4.2 区域构造响应

前已述及, 峨眉台地以及鸣条岗隆起晚更新世发生了明显的区域构造隆升, 导致了古汾河彻底退出运城盆地, 运城盆地原有的古汾河河道开始接受黄土沉积, 形成了明显的下部为河流相沉积、上部为黄土沉积的地层结构。那么该期构造隆升在区域上是否还有响应, 并且构造活动的动力机制如何, 需要结合已有研究资料加以讨论。

晚更新世中期 ($76.22 \pm 10.4 \sim 63.69 \pm 6.57$ ka) 发生的区域构造事件, 不仅在运城盆地, 而且涉及整个环鄂尔多斯盆地周缘, 在青藏高原东北缘弧形构造带的红寺堡盆地以及鄂尔多斯北缘的河套盆地都

有该期构造活动的沉积间断或地貌记录(李有利和杨景春, 1994; Jia et al., 2016, 2017; 崔加伟等, 2018; 黄婷等, 2018; 刘博华等, 2023)。在运城盆地, 晚更新世中期存在的区域不整合沉积以及运城盐湖盐矿层的形成时限, 都基本反应了该期构造运动与汾河改道之间的内在关系(李有利和杨景春, 1994; 胡小猛和杨景春, 2001)。运城盆地涑水平原王过村剖面晚更新世存在一角度不整合面, 根据此次光释光测年结果显示, 该期不整合面形成的时限大约为 6.7 万年左右。在北杨姚村剖面, 晚更新世丁村组与峙峪组岩性界面发生转换的时限介于 7.8~4.3 万年(图 7)。在运城盆地丁村组中, 发现了保存完好的厚蚌化石层, 这些厚壳河蚌仍保存着它们活着时候的状态, 多数个体还是左右壳完整地咬合在一起, 没有人为弃置和自然营力扰动的迹象, 完全没有被移动过, 属于原生堆积; 说明当时汾河古道突然干涸, 大规模的河蚌同时死亡, 上面的黄土很快覆盖了河道, 这些蚌类就被直接深埋在砂层中, 很好地保存了下来; 电子自旋共振(ESR)测年结果显示其化石层的形成时代大约为 7.8 万年(胡小猛和杨景春, 2001; 陈兴强等, 2016)。运城盐湖是上新世至早更新世三门古湖的残余, 早更新世末期黄河贯通三门峡, 三门古湖萎缩至运城盆地中条山山前的狭长凹陷内, 但此时古汾河河道流经运城盆地, 残余古湖通过古汾河河道与外界沟通, 并未完全形成封闭的湖盆, 直至晚更新世汾河完全退出运城盆地, 加之中条山北缘断裂的持续活动, 形成山前凹陷, 运城盐湖才真正的形成, 这也是运城盐湖的含盐层系主要存在于晚更新世至全新世地层中的原因(刘书丹等, 1988; 李有利和杨景春, 1994; 吴锡浩等, 1998; 潘保田等, 2005; Jiang et al., 2007; 杨守业等, 2001; 张磊等, 2018; Shang et al., 2018; 闫纪元等, 2021; 胡健民等, 2022)。青藏高原东北缘弧形构造带红寺堡盆地以及清水河盆地中, 晚更新世主要发育萨拉乌苏组与水洞沟组 2 套河湖相沉积, 二者之间存在 1 期明显的沉积间断, 沉积间断发生的时限为 7~5 万年之间(崔加伟等, 2018; 黄婷等, 2018; 李振宏等, 2020b; 马兆颖等, 2020; 董晓朋等, 2022, 2023)。鄂尔多斯盆地北缘河套盆地黄河阶地的研究表明, 5 万年左右为重要的河流阶地发育期, 该时期是河套盆地河流下切深度最大、相邻阴山造山带处于快速强烈隆升剥蚀的时期(Jia et al., 2016, 2017; 周青硕等, 2017)。综合运城盆地、青藏高原



a—尊村剖面; b—魏家园剖面 (闫纪元, 2021)

图 6 运城盆地碎屑锆石年龄序列对比

Fig. 6 Comparison of detrital zircon U-Pb age sequence in the Yuncheng Basin

(a) Sample from fluvial sands in the Zuncun section; (b) Sample from fluvial sands of the ancient Fen River in the Weijiayuan section (Yan, 2021)

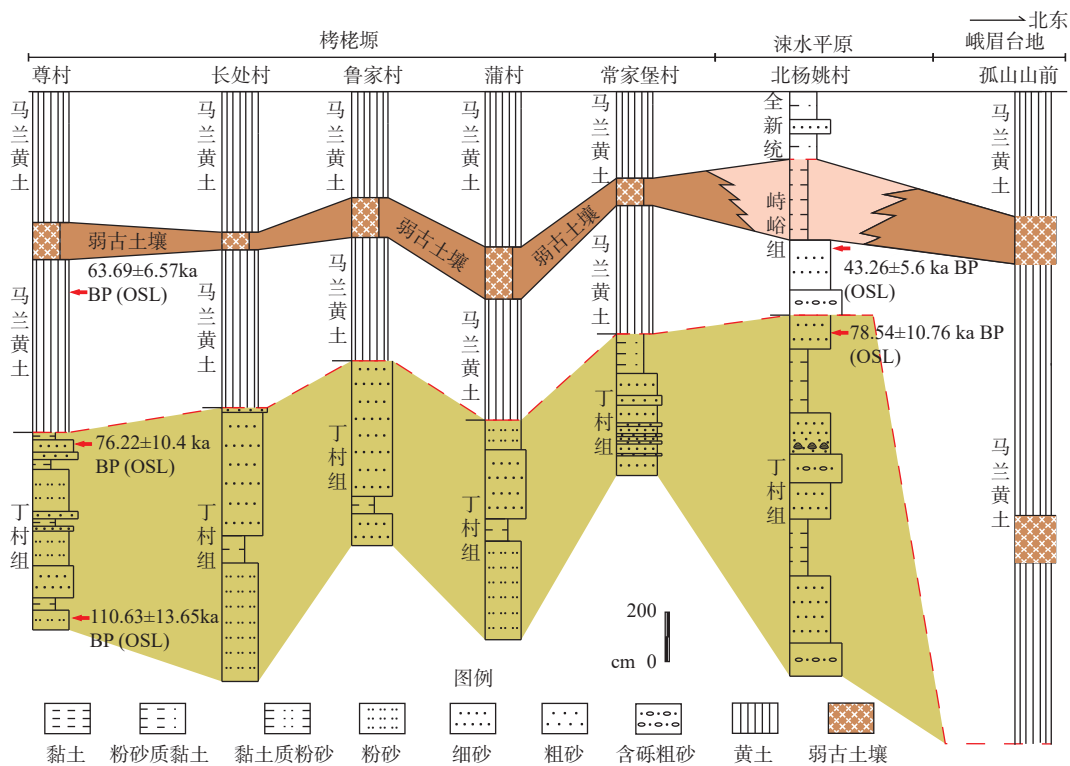


图 7 运城盆地晚更新世地层序列对比 (剖面位置见图 1)

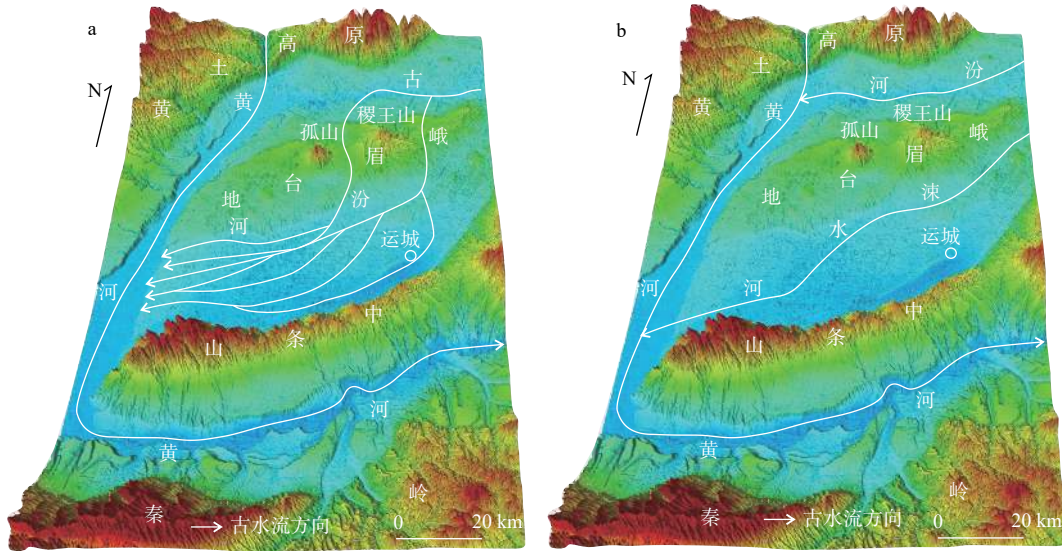
Fig. 7 Comparison of late Pleistocene stratigraphic sequences in the Yuncheng Basin (the location of the profile is shown in Fig. 1)

东北缘以及河套盆地构造、沉积、河流阶地以及灾变事件、盐湖成矿时限的研究成果, 可以发现鄂尔多斯盆地周缘大约在晚更新世中期均存在 1 期强烈的构造活动。该期构造活动的作用力主要来自于青藏高原隆升扩展的远程效应。数值模拟结果表

明, 运城盆地晚更新世至现今的构造应力场最大主压应力的优势方位为北东—北东东方向, 主要受到青藏高原向东北方向不断推挤作用的控制, 运动速率大小也有从鄂尔多斯盆地西南向北东方向逐渐递减的特征 (崔效锋等, 2010; 武敏捷等, 2011; 韩晓

明等, 2015; 林向东等, 2017; 仲启蒙等, 2022)。综合分析表明, 晚更新世中期青藏高原隆升扩展的远程效应造成鄂尔多斯周缘不同地区发生不均衡的抬升, 在运城盆地主要表现为峨眉台地与鸣条岗隆起

发生抬升, 从而造成了运城盆地河湖体系发生了明显的调整, 中更新世至晚更新世早期流经运城盆地的古汾河发生改道, 从此退出了运城盆地, 从现今的峨眉台地以北地区汇入黄河(图8)。



a—中更新世—晚更新世早期; b—晚更新世中期—全新世

图8 汾河古河道演化特征

Fig. 8 River courses evolution model of the ancient Fen River

(a) River courses of the ancient Fen River in the middle Pleistocene; (b) River courses of the ancient Fen River in the late Pleistocene

5 结论

(1) 运城盆地栲栳塬晚更新世具有下部为河流相、上部为风成黄土相的沉积序列, 二者之间的界限大约在7.6~6.3万年之间。

(2) 碎屑锆石年龄序列对比分析认为, 栲栳塬晚更新世早期的河流相为古汾河河道的残余沉积; 晚更新世中期, 峨眉台地与鸣条岗整体发生区域性抬升, 古汾河退出运城盆地, 废弃的古河道开始接受区域风成黄土沉积。

References

- AN Z S, LIU X D, 2000. History and variability of monsoon climate in East Asia[J]. *Chinese Science Bulletin*, 45(3): 238-249. (in Chinese)
- CHEN X Q, SHI W, HU J M, et al., 2016. Sedimentation of the Pliocene-Pleistocene Chaizhuang section in the central of Linfen Basin, North China and its tectonic significance[J]. *Journal of Geomechanics*, 22(4): 984-993. (in Chinese with English abstract)
- CUI J W, LI Z H, LIU F, et al., 2018. Redefinition of the sedimentary time of the Salawusu Formation in the Hongsibu Basin, Ningxia and its significance[J]. *Journal of Geomechanics*, 24(2): 283-292. (in Chinese with

English abstract)

- CUI X F, XIE F R, LI R S, et al., 2010. Heterogeneous features of state of tectonic stress filed in north china and deep stress in coal mine[J]. *Chinese Journal of Rock Mechanics and Engineering*, 29(S1): 2755-2761. (in Chinese with English abstract)
- DONG X P, LI Z H, CUI J W, et al., 2022. Discovery of periglacial phenomena in the late stage of Last Glacial Maximum at the upper to middle reaches of Qingshuihe River, Ningxia, China[J]. *Journal of Earth Sciences and Environment*, 44(3): 524-534. (in Chinese with English abstract)
- DONG X P, CUI J W, JIANG X H et al., 2023. Stratigraphic sequence characteristics and geochronology research progress of the Cenozoic in the arcuate tectonic belt in the northeastern Tibet Plateau[OL/J]. *Journal of Geomechanics*, DOI: 10.12090/j.issn.1006-6616.2023048. (in Chinese with English abstract)
- GUO L Z, XUE Y Q, 1958. The pleistocene sediments of the lower reaches of the Fenho and the Sushui: their origin and bearings on the geomorphological evolution of these two rivers[J]. *Quaternary Sciences*, 1(1): 107-117. (in Chinese)
- HAN H Y, MI F S, LIU H Y, 2001. Geomorphological structure in the Weihe Basin and neotectonic movement[J]. *Journal of Seismological Research*, 24(3): 251-257. (in Chinese with English abstract)
- HAN H Y, ZHANG Y, YUAN Z X, 2002. The evolution of Weihe down-faulted basin and the movement of the fault blocks[J]. *Journal of Seismological Research*, 25(4): 362-368. (in Chinese with English abstract)

- HAN X M, LIU F, ZHANG W T, et al., 2015. Analyzing the variation characteristics of stress field in Hetao seismic belt using focal mechanism data[J]. *Seismology and Geology*, 37(4): 1030-1042. (in Chinese with English abstract)
- HU J M, YAN J Y, CHENG Y, et al., 2022. Geological records of late Cenozoic tectono-sedimentary-paleoclimatic events in China[J]. *Geology and Resources*, 31(3): 303-330. (in Chinese with English abstract)
- HU X M, 1997. The change of former Fen river on EMEI platform[J]. *Journal of Anhui Normal University (Natural Science)*, 20(2): 154-158. (in Chinese with English abstract)
- HU X M, YANG J C, 2001. The evolution and its contributing factors of Linfen Basin since middle Quaternary[J]. *Journal of Shanghai Teachers University (Natural Sciences)*, 30(3): 72-76. (in Chinese with English abstract)
- HU X M, GUO J X, HU X Y, 2010. The development of Morpho-sediment of Quaternary in Fenhe River graben basins and the neotectonic movement[J]. *Acta Geographica Sinica*, 65(1): 73-81. (in Chinese with English abstract)
- HU X M, CHEN M J, WANG D T, et al., 2012. The Sequence difference in the times in the geomorphic-sedimentary evolution in the Fenwei graben basins during the middle-late Quaternary and its tectonic significance[J]. *Quaternary Sciences*, 32(5): 849-858. (in Chinese with English abstract)
- HUANG T, LI Z H, LIU F, et al., 2018. The current situation of desertification in the Hongsibu Basin, Ningxia, and its main geological controlling factors[J]. *Journal of Geomechanics*, 24(4): 505-514. (in Chinese with English abstract)
- JIA L Y, ZHANG X J, YE P S, et al., 2016. Development of the alluvial and lacustrine terraces on the northern margin of the Hetao Basin, Inner Mongolia, China: implications for the evolution of the Yellow River in the Hetao area since the late pleistocene[J]. *Geomorphology*, 263: 87-98.
- JIA L Y, HU D G, WU H H, et al., 2017. Yellow River terrace sequences of the Gonghe-Guide section in the northeastern Qinghai-Tibet: implications for plateau uplift[J]. *Geomorphology*, 295: 323-336.
- JIANG F C, FU J L, WANG S B, et al., 2007. Formation of the Yellow River, inferred from loess-palaeosol sequence in Mangshan and lacustrine sediments in Sanmen Gorge, China[J]. *Quaternary International*, 175(1): 62-70.
- JIN H L, LI M Q, SU Z Z, et al., 2006. Climatic change reflected by Stratigraphical magnetic susceptibility in Salawusu River basin, North China since 220 ka BP[J]. *Journal of Desert Research*, 26(5): 680-686. (in Chinese with English abstract)
- JIN H L, LI M Q, SU Z Z, et al., 2007. Sedimentary age of strata in the Salawusu River Basin and climatic changing[J]. *Acta Geologica Sinica*, 81(3): 307-315. (in Chinese with English abstract)
- LI S Z, YU S, ZHAO S J, et al., 2013. Tectonic transition and plate reconstructions of the east Asian continental margin[J]. *Marine Geology & Quaternary Geology*, 33(3): 65-94. (in Chinese with English abstract)
- LI S Z, CAO X Z, WANG G Z, et al., 2019. Meso-Cenozoic tectonic evolution and plate reconstruction of the Pacific Plate[J]. *Journal of Geomechanics*, 25(5): 642-677. (in Chinese with English abstract)
- LI Y L, YANG J C, 1994. Environmental evolution of Yuncheng daline lake (Shanxi, China)[J]. *Geographical Research*, 13(1): 70-74. (in Chinese with English abstract)
- LI Y L, YANG J C, SU Z Z, 1994. Neotectonic movement and palaeochannel evolution in Yuncheng Basin[J]. *Earthquake Research in Shanxi*(1): 3-6. (in Chinese with English abstract)
- LI Z C, LI W H, LI Y X, et al., 2015. Sedimentary facies of the Cenozoic in Weihe Basin[J]. *Journal of Palaeogeography*, 17(4): 529-540. (in Chinese with English abstract)
- LI Z C, LI W H, LI Y X, et al., 2016. Cenozoic stratigraphy and Paleoenvironments in the Weihe area, Shaanxi Province[J]. *Journal of Stratigraphy*, 40(2): 168-178. (in Chinese with English abstract)
- LI Z H, JIANG B Y, DONG X P, et al., 2020a. Collapses of loess at the front of the Emei tableland in the Yuncheng basin and their major geological controlling factors[J]. *Coal Geology & Exploration*, 48(2): 171-178. (in Chinese with English abstract)
- LI Z H, CUI J W, LI C Z, et al., 2020b. Late Pleistocene sedimentary features and the palaeoclimatic background in Hongsibao Basin[J]. *Coal Geology & Exploration*, 48(6): 233-242. (in Chinese with English abstract)
- LI Z Y, LI Y X, LI W H, et al., 2021. Sedimentary characteristics of Paleogene-Neogene in Fenwei Basin[J]. *Chinese Journal of Geology*, 56(4): 1120-1133. (in Chinese with English abstract)
- LIN X D, YUAN H Y, XU P, et al., 2017. Zonational characteristics of earthquake focal mechanism solutions in North China[J]. *Chinese Journal of Geophysics*, 60(12): 4589-4622. (in Chinese with English abstract)
- LIU B H, WU F, ZHANG X J, et al., 2023. Late Pleistocene element geochemistry and its implications for environmental change in Hongsibu Basin, northeastern margin of Qinghai-Tibet Plateau[J/OL]. *Geological Bulletin of China*: 1-16[2023-08-11]. <http://kns.cnki.net/kcms/detail/11.4648.P.20230811.1039.002.html>. (in Chinese with English abstract)
- LIU S D, LI G K, LI Y X, et al., 1988. Discussion on the formation and evolution of the Yellow River from the characteristics of Quaternary sediments in the eastern plain of Henan Province[J]. *Henan Geology*, 6(2): 20-24. (in Chinese)
- LIU Y S, HU Z C, GAO S, et al., 2008. *In situ* analysis of major and trace elements of anhydrous minerals by LA-ICP-MS without applying an internal standard[J]. *Chemical Geology*, 257(1-2): 34-43.
- LIU Y S, GAO S, HU Z C, et al., 2010a. Continental and oceanic crust recycling-induced melt-peridotite interactions in the Trans-North China Orogen: U-Pb dating, Hf isotopes and trace elements in zircons from mantle xenoliths[J]. *Journal of Petrology*, 51(1-2): 537-571.
- LIU Y S, HU Z C, ZONG K Q, et al., 2010b. Reappraisal and refinement of zircon U-Pb isotope and trace element analyses by LA-ICP-MS[J]. *Chinese Science Bulletin*, 55(15): 1535-1546.
- LUDWIG K R, 2003. ISOPLLOT 3.00: A geochronological toolkit for Microsoft excel[M]. Berkeley, California: Berkeley Geochronology Center: 39.
- MA Z Y, DONG X P, ZHANG Q, et al., 2020. Sedimentary response to the uplift of the Liupan Shan since the Late Pleistocene and its environmental effects[J]. *Coal Geology & Exploration*, 48(5): 152-164. (in Chinese with English abstract)
- PAN B T, WANG J P, GAO H S, et al., 2005. Paleomagnetic dating of the topmost terrace in Kouma, Henan and its indication to the Yellow River's

- running through Sanmen Gorges[J]. *Chinese Science Bulletin*, 50(7): 657-664.
- QI Y, XU H B, ZHANG J X, et al., 2011. Geochemistry, geochronology and geological significance of Gufengshan granodiorite in Linfen Grabben basin[J]. *Geological Review*, 57(4): 565-573. (in Chinese with English abstract)
- QI Y, LUO J H, WU J D, et al., 2016. Geochemical and Sr-Nd-Pb isotopic composition of the Canfang and Gufengshan granodiorite plutons in central-southern North China[J]. *Acta Petrologica Sinica*, 32(7): 2015-2028. (in Chinese with English abstract)
- QIN B C, FANG W X, ZHANG J G, et al., 2021. Quaternary sedimentary sequence and sedimentary environment restoration in the Jinzhong Basin, Fenhe Rift Valley[J]. *Journal of Geomechanics*, 27(6): 1035-1050. (in Chinese with English abstract)
- QIU D W, GONG W B, YAN J Y, et al., 2021. Geological environment changes during the late Pleistocene-Holocene on the E'mei tableland in the northern Yuncheng basin, Shanxi Province: implications for the distribution of human settlements[J]. *Journal of Geomechanics*, 27(2): 326-338. (in Chinese with English abstract)
- SHANG Y, PRINS M A, BEETS C J, et al., 2018. Aeolian dust supply from the Yellow River floodplain to the Pleistocene loess deposits of the Mangshan Plateau, central China: Evidence from zircon U-Pb age spectra[J]. *Quaternary Science Reviews*, 182: 131-143.
- SUN J M, XU L L, 2007. River terraces in the Fenwei Graben, Central China, and the relation with the tectonic history of the India-Asia collision system during the Quaternary[J]. *Quaternary Sciences*, 27(1): 20-26. (in Chinese with English abstract)
- SUO Y H, LI S Z, DAI L M, et al., 2012. Cenozoic tectonic migration and basin evolution in East Asia and its continental margins[J]. *Acta Petrologica Sinica*, 28(8): 2602-2618. (in Chinese with English abstract)
- SUO Y H, LI S Z, CAO X Z, et al., 2017. Mesozoic-Cenozoic inversion tectonics of East China and its implications for the subduction process of the oceanic plate[J]. *Earth Science Frontiers*, 24(4): 249-267. (in Chinese with English abstract)
- WANG Q, LI C G, TIAN G Q, et al., 2000. Great changes of surface system and tectonic setting of salt lake formation in Yuncheng Basin since 7.1 Ma[J]. *Science in China (Series D)*, 30(4): 420-428. (in Chinese)
- WIEDENBECK M, ALLÉ P, CORFU F, et al., 1995. Three natural zircon standards for U-Th-Pb, Lu-Hf, trace element and REE analyses[J]. *Geo-standards Newsletter*, 19(1): 1-23.
- WU M J, LIN X D, XU P, 2011. Analysis of focal mechanism and tectonic stress field features in northern part of north China[J]. *Journal of Geodesy and Geodynamics*, 31(5): 39-43. (in Chinese with English abstract)
- WU X H, JIANG F C, WANG S M, et al., 1998. On problem of the Yellow River passing through the Sanmen Gorge and flowing east into sea[J]. *Quaternary Sciences*, 18(2): 188. (in Chinese with English abstract)
- XING Z Y, ZHAO B, TU M Y, et al., 2005. The formation of the Fenwei rift valley[J]. *Earth Science Frontiers*, 12(2): 247-262. (in Chinese with English abstract)
- XU H L, WANG C D, 2010. Preliminary study on the relationship between the Fluvial geomorphology and the Neotectonic movement in Yellow River in Zhengzhou prehistoric times[J]. *Journal of North China Institute of Water Conservancy and Hydroelectric Power*, 31(6): 101-106. (in Chinese with English abstract)
- YAN J Y, 2021. Late Cenozoic tectonic-sedimentary, uplifting and denudation process of the Yuncheng Basin and northern Gushan Mountain[D]. Beijing: Chinese Academy of Geological Sciences. (in Chinese with English abstract)
- YAN J Y, HU J M, WANG D M, et al., 2021. The critical geological events in the Huang-Huai-Hai Plain during the Late Cenozoic[J]. *Geological Bulletin of China*, 40(5): 623-648. (in Chinese with English abstract)
- YANG S Y, CAI J G, LI C X, et al., 2001. New discussion about the run-through time of the Yellow River[J]. *Marine Geology & Quaternary Geology*, 21(2): 15-20. (in Chinese with English abstract)
- YAO W B, JI X Q, ZHAO Z, 2004. Sedimental features of loess in Yuncheng basin[J]. *Shanxi Architecture*, 30(9): 23-24. (in Chinese with English abstract)
- ZHANG L, LIU J Q, QIN X G, 2018. The environmental effects and mechanism of the Yellow River flooding into the Huabei Plain during Quaternary: a brief review[J]. *Quaternary Sciences*, 38(2): 441-453. (in Chinese with English abstract)
- ZHONG Q M, SHAO B, HOU G T, 2022. Numerical simulation and analysis of lithospheric stress field in Fenwei graben[J]. *Progress in Geophysics*, 37(1): 152-163. (in Chinese with English abstract)
- ZHOU Q S, ZHANG X J, YE P S, et al., 2017. The distribution and period division of Holocene palaeo channels of the Yellow River in Hetao area[J]. *Journal of Geomechanics*, 23(3): 339-347. (in Chinese with English abstract)

附中文参考文献

- 安芷生, 刘晓东, 2000. 东亚季风气候的历史与变率[J]. *科学通报*, 45(3): 238-249.
- 陈兴强, 施旸, 胡健民, 等, 2016. 华北临汾盆地中部柴庄上新世-更新世剖面沉积学特征及其构造意义[J]. *地质力学学报*, 22(4): 984-993.
- 崔加伟, 李振宏, 刘锋, 等, 2018. 宁夏红寺堡盆地萨拉乌苏组地层时代重新厘定及意义[J]. *地质力学学报*, 24(2): 283-292.
- 崔效锋, 谢富仁, 李瑞莎, 等, 2010. 华北地区构造应力场非均匀特征与煤田深部应力状态[J]. *岩石力学与工程学报*, 29(S1): 2755-2761.
- 董晓朋, 李振宏, 崔加伟, 等, 2022. 宁夏清水河中上游发现末次冰期最盛期冰缘遗迹群[J]. *地球科学与环境学报*, 44(3): 524-534.
- 董晓朋, 李振宏, 井向辉, 等, 2023. 青藏高原东北缘弧形构造带新生代地层沉积序列特征及年代学研究进展 [OL/J]. *地质力学学报*, DOI:10.12090/j.issn.1006-6616.2023048.
- 郭令智, 薛禹群, 1958. 从第四纪沉积物讨论山西汾河与涑水在地貌演化上的关系[J]. *第四纪研究*, 1(1): 107-117.
- 韩恒悦, 米丰收, 刘海云, 2001. 渭河盆地地貌结构与新构造运动[J]. *地震研究*, 24(3): 251-257.
- 韩恒悦, 张逸, 袁志祥, 2002. 渭河断陷盆地的形成演化及断块运动[J]. *地震研究*, 25(4): 362-368.
- 韩晓明, 刘芳, 张文韬, 等, 2015. 基于震源机制资料分析河套地震带的应力场变化特征[J]. *地震地质*, 37(4): 1030-1042.
- 胡健民, 闫纪元, 程瑜, 等, 2022. 中国晚新生代构造-沉积-古气候事

- 件的地质记录[J].地质与资源,31(3):303-330.
- 胡晓猛,1997.古汾河在峨嵋台上的变迁[J].安徽师范大学学报(自然科学版),20(2):154-158.
- 胡小猛,杨景春,2001.临汾盆地中更新世中晚期以来的演化历史及成因分析[J].上海师范大学学报(自然科学版),30(3):72-76.
- 胡小猛,郭家秀,胡向阳,2010.汾河地堑湖盆第四纪地貌-沉积特征的构造控制[J].地理学报,65(1):73-81.
- 胡小猛,陈美君,王杜涛,等,2012.汾渭地堑系列湖盆第四纪中晚期地貌与沉积阶段性演化的时间序次差异及其构造指示意义[J].第四纪研究,32(5):849-858.
- 黄婷,李振宏,刘锋,等,2018.宁夏红寺堡盆地地表沙漠化现状及地质主控因素[J].地质力学学报,24(4):505-514.
- 靳鹤龄,李明启,苏志珠,等,2006.220 ka 以来萨拉乌苏河流域地层磁化率与气候变化[J].中国沙漠,26(5):680-686.
- 靳鹤龄,李明启,苏志珠,等,2007.萨拉乌苏河流域地层沉积时代及其反映的气候变化[J].地质学报,81(3):307-315.
- 李三忠,余珊,赵淑娟,等,2013.东亚大陆边缘的板块重建与构造转换[J].海洋地质与第四纪地质,33(3):65-94.
- 李三忠,曹现志,王光增,等,2019.太平洋板块中-新生代构造演化及板块重建[J].地质力学学报,25(5):642-677.
- 李有利,杨景春,1994.运城盐湖沉积环境演化[J].地理研究,13(1):70-74.
- 李有利,杨景春,苏宗正,1994.运城盆地新构造运动与古河道演变[J].山西地震(1):3-6.
- 李智超,李文厚,李永项,等,2015.渭河盆地新生代沉积相研究[J].古地理学报,17(4):529-540.
- 李智超,李文厚,李永项,等,2016.陕西渭河地区新生代地层及沉积环境演化[J].地层学杂志,40(2):168-178.
- 李兆雨,李永项,李文厚,等,2021.汾渭盆地古近系-新近系沉积特征[J].地质科学,56(4):1120-1133.
- 李振宏,姜博宇,董晓朋,等,2020a.运城盆地峨眉台地前缘黄土塌陷现状及地质主控因素[J].煤田地质与勘探,48(2):171-178.
- 李振宏,崔加伟,李朝柱,等,2020b.红寺堡盆地晚更新世沉积特征及古气候背景[J].煤田地质与勘探,48(6):233-242.
- 林向东,袁怀玉,徐平,等,2017.华北地区地震震源机制分区特征[J].地球物理学报,60(12):4589-4622.
- 刘博华,吴芳,张绪教,等,2023.青藏高原东北缘红寺堡盆地晚更新世沉积物元素地球化学特征及其环境指示意义[J/OL].地质通报:1-16[2023-08-11].<http://kns.cnki.net/kcms/detail/11.4648.P.20230811.1039.002.html>.
- 刘书丹,李广坤,李玉信,等,1988.从河南东部平原第四纪沉积物特征探讨黄河的形成与演变[J].河南地质,6(2):20-24.
- 马兆颖,董晓朋,张庆,等,2020.六盘山晚更新世以来抬升过程沉积响应及环境效应[J].煤田地质与勘探,48(5):152-164.
- 潘保田,王均平,高红山,等,2005.河南扣马黄河最高级阶地古地磁年代及其对黄河贯通时代的指示[J].科学通报,50(3):255-261.
- 齐玥,徐鸿博,张竞雄,等,2011.临汾断陷盆地孤峰山花岗岩闪长岩的地球化学和年代学及其地质意义[J].地质论评,57(4):565-573.
- 齐玥,罗金海,巫嘉德,等,2016.华北中南部蚕坊和孤峰山花岗岩闪长岩体的地球化学特征和 Sr-Nd-Pb 同位素组成[J].岩石学报,32(7):2015-2028.
- 秦帮策,方维萱,张建国,等,2021.汾河裂谷晋中盆地内第四纪沉积序列与沉积环境恢复[J].地质力学学报,27(6):1035-1050.
- 仇度伟,公王斌,闫纪元,等,2021.山西运城盆地北部峨嵋台地晚更新世-全新世地质环境变化及其对人类聚落分布的影响[J].地质力学学报,27(2):326-338.
- 孙继敏,许立亮,2007.汾渭地堑的河流阶地对第四纪时期印度-欧亚板块碰撞带的构造响应[J].第四纪研究,27(1):20-26.
- 索艳慧,李三忠,戴黎明,等,2012.东亚及其大陆边缘新生代构造迁移与盆地演化[J].岩石学报,28(8):2602-2618.
- 索艳慧,李三忠,曹现志,等,2017.中国东部中生代反转构造及其记录的大洋板块俯冲过程[J].地学前缘,24(4):249-267.
- 王强,李彩光,田国强,等,2000.7.1Ma 以来运城盆地地表系统巨变及盐湖形成的构造背景[J].中国科学(D辑),30(4):420-428.
- 武敏捷,林向东,徐平,2011.华北北部地区震源机制解及构造应力场特征分析[J].大地测量与地球动力学,31(5):39-43.
- 吴锡浩,蒋复初,王苏民,等,1998.关于黄河贯通三门峡东流入海问题[J].第四纪研究,18(2):188.
- 邢作云,赵斌,涂美义,等,2005.汾渭裂谷系与造山带耦合关系及其形成机制研究[J].地学前缘,12(2):247-262.
- 徐海亮,王朝栋,2010.史前郑州地区黄河河流地貌与新构造活动关系初探[J].华北水利水电学院学报,31(6):101-106.
- 闫纪元,2021.运城盆地及北侧孤山晚新生代构造-沉积与隆升-剥蚀过程研究[D].北京:中国地质科学院.
- 闫纪元,胡健民,王东明,等,2021.黄淮海平原晚新生代重大地质事件[J].地质通报,40(5):623-648.
- 杨守业,蔡进功,李从先,等,2001.黄河贯通时间的新探索[J].海洋地质与第四纪地质,21(2):15-20.
- 姚文兵,季秀卿,赵政,2004.运城盆地黄土沉积特征[J].山西建筑,30(9):23-24.
- 张磊,刘嘉麒,秦小光,2018.第四纪黄河入淮成因机制与环境效应的研究现状及存在问题[J].第四纪研究,38(2):441-453.
- 仲启蒙,邵博,侯贵廷,2022.汾渭地堑岩石圈的应力场数值模拟与分析[J].地球物理学进展,37(1):152-163.
- 周青硕,张绪教,叶培盛,等,2017.河套地区全新世黄河古河道的分布及期次划分[J].地质力学学报,23(3):339-347.